Developmental Cognitive Neuroscience 60 (2023) 101202

Contents lists available at ScienceDirect

Developmental Cognitive Neuroscience

journal homepage: www.elsevier.com/locate/dcn

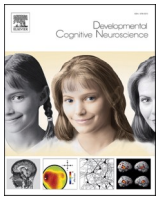

Preterm birth and neonatal white matter microstructure in in-vivo reconstructed fiber tracts among audiovisual integration brain regions

Juan F. Quinones [a,b,*], Andrea Hildebrandt [a,b,c,*], Tommaso Pavan [f], Christiane M. Thiel [b,c,e], Axel Heep [c,d]

[a] Psychological Methods and Statistics, Department of Psychology, School of Medicine and Health Sciences, Carl von Ossietzky Universität Oldenburg, Oldenburg, Germany
[b] Cluster of Excellence Hearing4all, Carl von Ossietzky Universität Oldenburg, Oldenburg, Germany
[c] Research Center Neurosensory Science, Carl von Ossietzky Universität Oldenburg, Germany
[d] Klinik für Neonatologie, Intensivmedizin und Kinderkardiologie, Oldenburg, Germany
[e] Biological Psychology, Department of Psychology, School of Medicine and Health Sciences, Carl von Ossietzky Universität Oldenburg, Oldenburg, Germany
[f] Department of Radiology, Lausanne University Hospital (CHUV) and University of Lausanne (UNIL), Lausanne, Switzerland

ARTICLE INFO

Keywords:
Audiovisual integration
Neonates
Preterm
Structural connectivity
DTI
NODDI

ABSTRACT

Individuals born preterm are at risk of developing a variety of sequelae. Audiovisual integration (AVI) has received little attention despite its facilitating role in the development of socio-cognitive abilities. The present study assessed the association between prematurity and in-vivo reconstructed fiber bundles among brain regions relevant for AVI. We retrieved data from 63 preterm neonates enrolled in the Developing Human Connectome Project (http://www.developingconnectome.org/) and matched them with 63 term-born neonates from the same study by means of propensity score matching. We performed probabilistic tractography, DTI and NODDI analysis on the traced fibers. We found that specific DTI and NODDI metrics are significantly associated with prematurity in neonates matched for postmenstrual age at scan. We investigated the spatial overlap and developmental order of the reconstructed tractograms between preterm and full-term neonates. Permutation-based analysis revealed significant differences in dice similarity coefficients and developmental order between preterm and full term neonates at the group level. Contrarily, no group differences in the amount of interindividual variability of DTI and NODDI metrics were observed. We conclude that microstructural detriment in the reconstructed fiber bundles along with developmental and morphological differences are likely to contribute to disadvantages in AVI in preterm individuals.

1. Introduction

Preterm (PT) birth is defined as delivery occurring before 37 completed weeks of gestation (Thorgeirsson et al., 1979). In clinical practice, three prematurity groups are differentiated according to gestational age (GA) at birth: PT (between 37 and 31 weeks), very preterm (vPT; between 31 and 28 weeks) and extremely preterm (ePT; <28 weeks). Approximately 11% of all worldwide deliveries occur prematurely, corresponding to roughly 15 million infants born every year (Pascal et al., 2018). Prematurity has been linked to cognitive, developmental and learning difficulties (including impaired vision and hearing loss [Mwaniki et al., 2012]), which may occur without evident brain alterations (Miller and Ferriero, 2009) and whose prevalence has been associated with increasing prematurity (Pascal et al., 2018). Given great progress in perinatal care, research on prematurity has shifted from quantifying mortality and physical morbidities to understanding neural correlates of motor (Coker-Bolt et al., 2016; Navarra et al., 2016; Pavaine et al., 2016), sensory-perceptual (Monson et al., 2018; Weinstein et al., 2016) and cognitive sequelae (e.g., Bartha-Doering et al., 2019; Caldinelli et al., 2017; Fenoglio et al., 2017; Jansson-Verkasalo et al., 2010; Kerr-Wilson et al., 2012; Loe et al., 2019). Audiovisual integration (AVI) remains comparably unattended, despite being related to cognitive and emotional development and social cognition (Mileva et al., 2018). Specifically, the ability to combine auditory and visual stimuli into a unified percept entails developmental advantages in several cognitive domains, for instance in language

* Correspondence to: Carl von Ossietzky Universität Oldenburg, Department of Psychology, Ammerländer Heerstr., 114-11, 826129 Oldenburg, Germany.
E-mail addresses: juan.felipe.quinones.sanchez@uni-oldenburg.de (J.F. Quinones), andrea.hildebrandt@uni-oldenburg.de (A. Hildebrandt).

https://doi.org/10.1016/j.dcn.2023.101202
Received 25 August 2022; Received in revised form 2 January 2023; Accepted 25 January 2023
Available online 27 January 2023

(Altvater-Mackensen and Grossmann, 2015; Teinonen et al., 2008), attention (Curtindale et al., 2019), affect discrimination (Flom and Bahrick, 2012) and social cognition (Grossmann, 2015). Furthermore, AVI has been linked to disorders such as dyslexia (Yang et al., 2020). Thus, impaired AVI likely contributes to a widespread of short- and long-term sequelae following PT birth (e.g., Elburg and Oosterlaan, 2019; Healy et al., 2013; Jones et al., 2013; Loe et al., 2019; Stipdonk et al., 2018). The scaffolding nature of this ability urges researchers to study it from the beginning of the life span onwards.

Behavioral studies discovered an association between prematurity and different forms of AVI during the first year of life. For example, native speech discrimination and face-voice synchrony preference is negatively associated with PT birth (Berdasco-Muñoz et al., 2019; Imafuku et al., 2019; Pickens et al., 1994). A handful of functional studies have elucidated brain regions engaged in AV processing in term-born infants shortly after birth. These include the superior temporal sulcus (STS), superior temporal gyrus, primary visual and auditory areas and portions of the frontal and parietal lobes (Altvater-Mackensen and Grossmann, 2016; Bristow et al., 2009; Fellman et al., 2004; Kushnerenko et al., 2008; Sours et al., 2017), as well as functional connectivity among them (Sours et al., 2017). Regarding structural connectivity, Quinones et al. (2022) traced connections among these and additional brain regions relevant for AVI (Hickok et al., 2018; Zhou et al., 2020) and compared them to those analogously traced in an adult sample. The study concluded that some AVI connections in neonates are likely to represent meaningful structural pathways, as in adults. Importantly, structural connectivity among some of these brain regions are associated with AVI performance in adults (Møller et al., 2021; Zamm et al., 2014). This suggests that individual differences in AVI depend on structural connectivity among some of these brain regions, at least to a certain extent. To our knowledge, no study has explicitly investigated how prematurity relates to structural or functional connectivity among the aforementioned AVI relevant brain regions early in life. Here, we aim to fill some of these gaps by investigating the association of prematurity with structural connectivity in the neonatal brain among brain regions previously shown to be activated during AVI tasks. We focused on microstructural models considering their sensitivity to detect white matter developmental changes.

Diffusion tensor imaging (DTI) studies have shown qualitatively similar developmental patterns of the white matter in full term (FT) and PT individuals (Faria et al., 2010; Gao et al., 2009; Geng et al., 2012; Kersbergen et al., 2014; Kidowaki et al., 2017; Miller et al., 2002; Nossin-Manor et al., 2015). That is, whereas fractional anisotropy (FA) generally increases with age, axial diffusivity (AD), mean diffusivity and radial diffusivity (RD) tend to decrease. Similar patterns were observed in tracts reconstructed among AVI regions in term-born neonates (Quinones et al., 2022). In quantitative terms however, prematurity has been associated with developmental delays in certain brain regions, for instance the corpus callosum and association fibers (Akazawa et al., 2016; Baldoli et al., 2015; Jo et al., 2012; Rose et al., 2008).

Neurite orientation dispersion and density imaging (NODDI) has been proposed to improve the characterization of brain tissue relative to DTI by adopting a model that differentiates three microstructural environments (Kamiya et al., 2020; Zhang et al., 2012). A recent study employing this technique on healthy individuals described a rapid increase in the neurite density index (NDI) from the first months of life and reported weak negative correlations between the orientation dispersion index (ODI) and age (Lynch et al., 2020). Similarly, Kimpton et al. (2021) reported significant positive correlations between NDI and post-menstrual age (PMA) at scan in several white matter pathways, for instance the corticospinal tract (Kimpton et al., 2021). In contrast, ODI in these white matter tracts was not significantly associated with PMA. Overall, neurodevelopmental studies applying NODDI suggest that an increase in NDI is a marker of development, whereas ODI remains stable over several years following birth (Kamiya et al., 2020).

1.1. Aims of the present study

Here we aim to study the association of prematurity with microstructural properties of reconstructed fiber bundles connecting brain areas reported to be relevant for AVI. In line with the literature pointing to differences between FT and PT infants in terms of white matter development, we postulated four hypotheses: 1) We expect a significant association between GA at birth (indicating the extent of prematurity) and DTI and NODDI metrics in a sample of PT and FT neonates matched for PMA at scan. Given the above summarized literature about developmental trajectories of DTI and NODDI metrics, the associations with GA is expected to be positive for FA and NDI, but negative for AD and RD. 2) Given a more variable GA at birth and more prolonged extrauterine exposure in PT as compared with FT neonates, we postulate higher interindividual differences in the microstructural properties of the reconstructed fiber bundles in PT neonates. 3) Due to the interruption of typical in-gestation processes, we further expect differences in the developmental order of reconstructed fiber bundles linking brain regions associated with AVI in FT and PT infants and 4) in their morphology. In summary, the present work aims to improve our understanding of structural brain connectivity among brain regions reported to be engaged in AVI early in life and its relationship with PT birth.

2. Materials and methods

2.1. Participants

Participants were sampled from the second data release of the Developing Human Connectome Project (dHCP; http://www.developingconnectome.org/project/), which contains over 500 data sets from infants born and scanned between 24 and 45 weeks of age. Main exclusion criteria were health conditions unsuitable for MRI scanning despite neonatal care. The study was approved by the Research Ethics Committee reference number: 14/LO/1169 of the UK Health Research Authority and parental written consent for imaging procedures and data release was given. Quality checks were conducted at five different stages by dHCP experts, including during-scan notes, visual inspection of images and modality-specific metrics derived from the data processing pipelines. Final decisions for data release relied on different combinations of failing or passing these checks. We sampled data sets if both structural and diffusion weighted imaging (DWI) scans were available and complete to allow application of NODDI. The sampling was further based on radiological scores, which should be less or equal to 4 (N = 361). Criteria for computing radiological scores were the presence of incidental findings with or without potential significance for clinical purposes or data analysis. For a complete description of the dHCP recruiting and rating procedures, see the dHCP's project documentation (http://www.developingconnectome.org/project/).

Next, all available PT infants whose tractography analysis, DTI and NODDI successfully concluded (N = 63) were matched with FT infants on a 1:1 basis according to the covariates sex assigned at birth, PMA at scan and radiological scores. Propensity scores were used for matching (Austin, 2011). This method balanced the density of observations along the variable GA and accounted for PT vs. FT differences depending on the covariates, especially PMA at scan. More specifically, matching 1:1 results in considering only a subset of the available FT observations, but it allows best mitigating the covariate-induced bias between the subsamples and reduces the imbalance in variance across the range of GA at birth in this specific dataset in which FT neonates were oversampled. This is favorable for the planed regression and linear spline analysis (see Section 2.5) because it secures equivalent density of cases along GA and facilitates homoscedasticity. The final sample included $N1$ = 126 neonates (63 PT infants, including vPT and ePT). Additional sample information is summarized in Table 1. Because the transformation file required for the analysis aiming to test the fourth hypothesis (see Section

Table 1
Demographic information of the neonates included in the first sample.

Group	Assigned sex at birth	*N1*	GA birth	PMA scan	RS	Weight	HC	EE
FT	F	23	39.75 (1.13)	40.66 (1.29)	2.35 (0.78)	3.43 (0.51)	34.97 (1.65)	0.91 (1.08)
FT	M	40	39.78 (1.3)	40.72 (1.69)	2.05 (0.85)	3.38 (0.49)	34.87 (1.57)	0.94 (1.14)
PT	F	18	34.56 (2.01)	40.74 (2.75)	2.72 (0.46)	2.09 (0.68)	34.68 (1.96)	6.17 (3.59)
PT	M	25	34.47 (1.89)	39.94 (1.74)	1.8 (0.87)	2.32 (0.6)	35.02 (1.71)	5.47 (2.73)
vPT	F	5	29.77 (0.81)	41.17 (0.94)	1.4 (0.55)	1.12 (0.28)	34.68 (1.16)	11.4 (1.55)
vPT	M	8	28.96 (0.83)	40.5 (1.71)	2.62 (0.74)	1.1 (0.23)	33.15 (3.4)	11.54 (1.76)
ePT	F	2	25.86 (0.4)	41.29 (0.61)	2.5 (0.71)	0.86 (0.12)	34.55 (0.07)	15.43 (0.2)
ePT	M	5	26.57 (1.25)	41.8 (1.77)	2.4 (0.89)	0.8 2(0.22)	34.26 (2.33)	15.23 (2.26)

Note. GA – Gestational age in weeks; PMA – Postmenstrual age in weeks; RS – Radiological score; HC – head circumference in cm; EE – Extrauterine exposure: Weeks elapsed between delivery and scan; Weight – Weight at birth in Kg. FT – full term; PT – preterm; vPT – very preterm; ePT – extremely preterm; F – female at birth; M – male.

2.4.3) were missing for several of the individual data sets included in the above mentioned matched sample, we repeated the matching procedure described above based on PT and FT neonates for whom the transformation file was available and the tractography was successful. Because for this analysis DTI and NODDI files were not a requirement, this procedure led to a slightly larger second sample (*N2* = 132, PT = 66; see Table 2), which overlapped with the first one by 88%.

2.2. MRI data acquisition and preprocessing

2.2.1. Acquisition

MRI scans were acquired at the Evelina Newborn Imaging Centre, St Thomas' Hospital, London, UK using a dedicated neonatal imaging system with a 32 channel head coil and a 3 T Philips Achieva MRI scanner. Individual scanning sessions consisted of structural (T1w and T2w), resting-state fMRI and diffusion MRI scans. T2w (TR = 12000, TE = 156 ms) and inversion recovery T1w (TR = 4795, TE = 8.7 ms) multi-slice fast spin-echo images were acquired in sagittal and axial slice stacks. Each slice was 1.6 mm thick with an in-plane resolution of 0.8 × 0.8 mm^2 and an overlap of 0.8 or 0.74 mm. For the acquisition of diffusion MRI data, four subsets of directions (one for each phase encoding direction) on four shells with b-values of 0, 400, 1000 and 2600 were used. The acquisition sequence (TR = 3800, TE = 90 ms) was customized such that it could be resumed if interrupted. In-plane image resolution was 1.5 × 1.5 mm^2 with 3 mm thickness slices and 1.5 mm overlap. More detailed imaging protocol descriptions can be accessed via the official dHCP documentation and publications on the dHCP data processing (e.g., Bastiani et al., 2019; Makropoulos et al., 2018).

2.2.2. Preprocessing

We made use of preprocessed structural and DWI data provided by the dHCP. The preprocessing pipelines were purposely designed to address the challenges of neonatal MRI and are fully described by the dHCP experts. The pipeline for intended structural analyses (Makropoulos et al., 2018) covers five major steps: Initially, anatomical scans are reconstructed. Then, the tissue is segmented and labeled accordingly. Next, white matter and pial surfaces are extracted and inflated to different scales for visualization or processing purposes. Lastly, descriptors of cortical features are estimated, for instance myelination maps and sulcal depth. For the present analyses we used participants' anatomical scans, pial and white matter surfaces, sphere surfaces and sulcal depth measures. The DWI preprocessing pipeline (Bastiani et al., 2019) selects a subset of b0 volumes and estimates the fieldmap. Then, correction for eddy currents, susceptibility induced distortions and motion is performed. A super-resolution algorithm is applied, followed by registration between diffusion and anatomical scans in native space. Both structural and diffusion MRI pipelines may be accessed and ran locally by users (see https://github.com/BioMedIA/dhcp-structural-pipeline).

2.3. Microstructural models

To assess microstructural properties of brain tissue we applied the DTI and NODDI models. DTI was performed on the preprocessed DWI data using the FDT toolbox in the FMRIB Software Library (FSL version 6.0.3; fsl.fmrib.ox.ac.uk/). The resulting scalars relate to the amount of water molecules diffusion parallel or perpendicular to the principal eigenvector of the tensor (AD and RD, respectively) or the mean diffusivity (MD). FA is a normalized measure of the amount of anisotropic diffusion relative to the overall diffusion and has long been used as a marker of fiber integrity (O'Donnell and Westin, 2011). We used the Diffusion Microstructure Imaging Toolbox in Python (Dmipy; Fick et al., 2019) to fit the NODDI-Bingham model (Tariq et al., 2016) to the preprocessed DWI data. Resulting metrics considered here are the ODI, representing how aligned or isotropic fibers are and the NDI, indicating density of neurites (volume fraction of neurites), typically representing axons and dendrites (Fukutomi et al., 2019; Kamiya et al., 2020; Mccunn et al., 2019).

2.4. Regions of interest and fiber tracing

2.4.1. AVI regions of interest

We followed the procedure implemented in Quinones et al. (2022) to define ROIs involved in AVI. In brief, we applied the publicly accessible

Table 2
Demographic information of the neonates included in the second sample.

Group	Assigned sex at birth	*N2*	GA birth	PMA scan	RS	Weight	HC	EE
FT	F	24	39.72(1.22)	40.8(1.68)	2.38(0.88)	3.32(0.59)	34.69(1.98)	1.08(1.2)
FT	M	42	39.89(1.26)	40.87(1.67)	2.1(0.98)	3.39(0.5)	34.94(1.76)	0.98(1.15)
PT	F	20	34.36(2.06)	40.96(2.76)	2.65(0.59)	2.05(0.7)	34.7(1.85)	6.59(3.8)
PT	M	24	34.46(1.94)	40.06(1.69)	1.71(0.86)	2.31(0.6)	35.14(1.62)	5.6(2.72)
vPT	F	6	29.79(0.72)	41.57(1.29)	1.33(0.52)	1.17(0.27)	34.98(1.28)	11.79(1.68)
vPT	M	9	28.86(0.84)	40.94(2.07)	2.78(0.83)	1.09(0.22)	33.52(3.37)	12.08(2.32)
ePT	F	2	25.86(0.4)	41.29(0.61)	2.5(0.71)	0.86(0.12)	34.55(0.07)	15.43(0.2)
ePT	M	5	26.57(1.25)	41.8(1.77)	2.4(0.89)	0.82(0.22)	34.26(2.33)	15.23(2.26)

Note. GA – Gestational age in weeks; PMA – Postmenstrual age in weeks; RS – Radiological score; HC – head circumference in cm; EE – Extrauterine exposure: Weeks elapsed between delivery and scan; Weight – Weight at birth in Kg. FT – full term; PT – preterm; vPT – very preterm; ePT – extremely preterm; F – female at birth; M – male.

shell scripts (see https://github.com/ecr05/dHCP_template_alignment) and performed a rigid registration between the neonates' anatomical scan and the 40-week anatomical template provided by the dHCP on the MIRTK software (https://mirtk.github.io/index.html). The resulting rotational estimates and rotational transforms provided by the dHCP experts were then used on the Connectome Workbench software version 1.2.3 (https://www.humanconnectome.org/software/connectome-workbench: Marcus et al., 2011) to bring each neonate's sphere surface into FreeSurfer space. The resulting sphere surface was then resampled on the Multimodal Surface Matching (MSM) software (Robinson et al., 2014, 2018) to match the resolution of the 40-week template sphere surface, which was in turn registered to the Human Connectome Project template sphere surface. The registration spheres obtained through the previous two non-linear registrations allowed us to map atlas labels from the cortical multimodal parcellation atlas (MMP; Glasser et al., 2016) onto neonatal native surfaces and anatomical scans (T2w). The MMP atlas parcellates each brain hemisphere into 180 regions by combining multimodal information. Individual ROIs may be merged to form larger areas. Following this principle, we defined 10 ROIs (see Fig. 1).

(requires color printing 2-column fitting image).

2.4.2. Fiber tracing

We applied a Bayesian Estimation of Diffusion Parameters obtained using Sampling Techniques (BEDPOSTX; see Behrens et al., 2007) to the preprocessed DWI data to generate voxel-wise distributions on diffusion parameters. Next, hemisphere-independent fiber tracing was performed using each ROI of a given fiber bundle as both seed and target. We kept default values for the major fiber tracing algorithm arguments (number of samples = 5000, length of samples = 0.5 mm, number of steps = 2000 and curvature threshold = 0.2) and included waypoint and waystop (e.g., midwall and pial surface) criteria to ensure retention of streamlines connecting both ROIs. The resulting bidirectional connectivity maps were thresholded with a robust-range threshold of 20% to remove false positive streamlines and multiplied with each other to obtain the overlapping region, which was then binarized. Finally, hemisphere-specific fiber bundle masks were aggregated and then used to estimate bihemispheric tract-constrained means of DTI and NODDI metrics for every neonate.

2.4.3. Fiber bundle mask aggregation

To compare tractograms in FT and PT participants spatially we created group-wise aggregated masks using data from the second sample included in this study (see section2.1). Transformation files provided in the dHCP data release were used to register individual fiber bundle masks to the standard dHCP template space. For FT and PT neonates independently, these individual transformed fiber bundle masks were aggregated and the resulting templates were thresholded using 10–90% relative thresholds and then binarized. This procedure resulted in 10 different versions of the same group-wise fiber bundle, representing the probability of spatial overlap of individual fiber bundle masks within FT and PT groups. At higher threshold levels, the spatial information is more specific and less likely to be contaminated with residual tractography results from inter-individual variation. We refer to these thresholded variants as specificity levels.

2.5. Statistical analysis

Statistical analyses were carried out in the **R** Software for Statistical Computing (R Core Team, 2022) version 4.2.1. The main **R** functions used are listed in Table A.1. Outliers in DTI and NODDI metrics were removed using as criterion 1.5 times the interquartile range exceeding upper and lower boundaries of itself.

Our first hypothesis, which postulated specific associations between the magnitude of prematurity and DTI/NODDI metrics, was statistically tested by means of a step-wise modeling approach with evolving model complexity. In a first stage, we employed single global linear regression models to predict all metrics of interests by the GA at birth. The simple linear model has two parameters (i.e., intercept and slope) and describes a linear relationship between GA and white matter property metrics. In a second stage, to investigate variability in these associations among differentiated prematurity age ranges (PT, vPT and ePT), linear regression splines – also known as segmented regression with fixed intercepts – were applied. In general, spline models are local and allow testing linear or curvilinear associations within theoretically defined or automatically

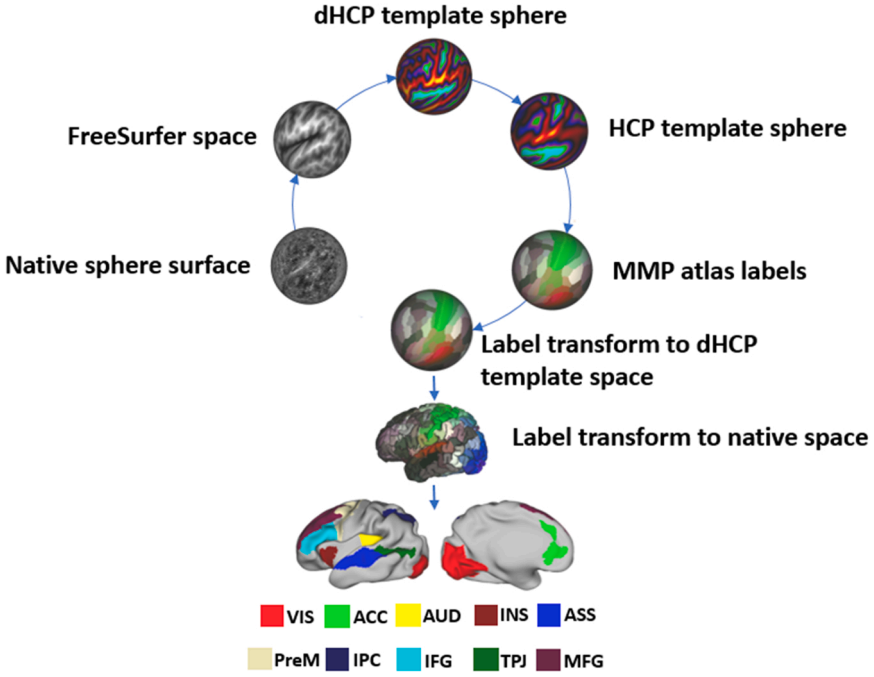

Fig. 1. Audiovisual integration ROIs. Main steps of ROI transformation, extraction and selection. VIS – visual cortices; AUD – auditory cortices; ASS –associative multisensory areas (along the STS); PreM – premotor cortex; MFG – middle frontal gyrus; ACC – anterior cingulate cortex; INS – anterior insula; IPC – inferior parietal cortex; IFG – inferior frontal gyrus; TPJ – temporo-parietal junction.

chosen bins of a predictor variable by aligning the predictions across the bins. We here applied linear functions within the bins. They capture bin-specific association patterns, thus avoiding to impose global assumptions about the shape of the association across the whole range of the independent variable (here GA at birth in neonates matched for PMA at scan). The selection of cut-off points (knots) is key in splines. There are two approaches for knot selection: data-driven or theoretical. We defined 28, 31 and 37 weeks of GA as knots given that these underlie the clinical classification of infants into prematurity groups. These clinically relevant cutoffs have a long tradition given that they reflect survival chances of premature neonates. Importantly, we did not use categorical regression to compare three groups of neonates because such an approach would eliminate within-bin individual differences. Instead, we were interested in continuous association measures between the magnitude of prematurity and the white matter fiber property metrics within the clinically defined groups of PT and FT neonates. We fitted linear, instead of curvilinear splines given that the visual inspection of the data did not suggest highly nonlinear associations between DTI and NODDI metrics and GA. There is also no theoretical reason to believe that within bin associations would follow a non-linear trajectory.

Our second hypothesis postulated substantial inter-individual differences between groups with larger variance in the PT group. To test this hypothesis, we compared DTI and NODDI metrics' variances between the FT and PT groups for all fiber tracts of interests by means of Levene tests. The procedure tests the null hypothesis of non-larger variances by conducting a *t*-test on group-wise absolute deviation scores.

To test the third hypothesis comparing the developmental order of fiber tracts between FT and PT groups, we computed intra-class correlation (ICC) coefficients between group-wise average scores resulting from the DTI and NODDI models. That is, first, group-wise average DTI and NODDI metrics were computed for each fiber tract. Second, we estimated the ICC for each metric of interest between these group-specific average scores across all reconstructed fiber tracts. The ICC is a measure of agreement in terms of rank orders between two quantitative variables, such that a large ICC coefficient would indicate similar rank position of fiber tracts' DTI and NODDI metrics between PT vs. FT neonates. We tested whether the computed ICC coefficients were significantly different from 1 (perfect ICC representing full agreement) by means of permutation tests. Null ICC coefficient distributions were simulated by randomly sampling individual observations from the entire data set and allocating them to pseudo PT vs. FT groups, repeating this procedure 500 times. Each time ICC coefficients are computed. Finally, empirical ICC coefficients are compared with the simulated distributions. Statistical significance is concluded based on the probability of obtaining an empirical result lying outside defined cut-offs of the null distribution created by the permutation. We chose.05 as the cut-off and a one-sided hypothesis.

Lastly, to test our fourth hypothesis, dice similarity coefficients (DSCs) between PT vs. FT groups were computed for each aggregated fiber tract template and specificity level (see Section 2.4.3.). DSCs are commonly used in radiology and MRI analysis (Yao et al., 2020) as a measure of spatial overlap (range: 0 meaning no overlap, 1 indicating total overlap) between images. Here, DSCs indicate the spatial correspondence between FT vs. PT neonates' aggregated tractograms, such that large vs. small DSCs represent spatial similarity vs. divergence, respectively. To test whether DSCs were statistically significant (i.e., substantially different from those obtain by sampling error), we simulated the null distribution by repeating the procedure described in Section 2.4.3. 500 times. In each repetition, pseudo PT vs. FT groups were created by randomly sampling observations from the joint data set and allocating them to either one. The significance of the empirical DSCs is given under the same criteria as for the ICC coefficients. Note that in order to test hypotheses 2–4, all neonates belonging to the different prematurity groups were labeled as PT.

2.6. Data and code availability statement

Preprocessed data analyzed in this study may be obtained via registration to the Developing Human Connectome Project (dHCP); http://www.developingconnectome.org/project/ and provided that access is granted by the project administrators. Scripts used to perform the neuroimaging and statistical analysis described in the method sections will be made publicly available at OSF (https://osf.io/24hcb/).

3. Results

3.1. Preterm birth and microstructural properties of AVI fiber tracts

Panel A of Fig. 2 depicts the reconstructed fiber bundles in the FT and PT groups of neonates. The results of linear and spline regression models for FA, MD, RD, ODI and NDI in one example fiber tract are illustrated in Panels B and C in Fig. 2. The results corresponding to the remaining fiber tracts and metrics of interest are provided in the supplementary material section (Table A.2). The linear models revealed a significant association between GA at birth and some of the DTI and NODDI metrics after matching for PMA at scan. Specifically, when scanned at around term age, higher FA and NDI are associated with higher GA at birth. On the other side, MD and RD are increasing with increasing prematurity (see negative associations displayed in Fig. 2.). Thus, prematurity is associated with lower tract-averaged anisotropic diffusion and neurite density. However, AD and ODI were not associated with GA at birth, and only little differences were observed in the present cross-sectional analyses for these metrics. To assess differences in DTI and NODDI metrics in a more elaborated manner among clinically-defined prematurity groups and FT neonates, we fitted a series of first-degree spline regression models (see Panel C in Fig. 2). These revealed within-bin and overall differences in microstructural properties as a function of GA at birth. Within-bin differences in the magnitude of the linear slope were overlooked by global models. Notably, the slope of the linear function that corresponds to the bin of ePT neonates is much steeper in the linear spline regression models as compared with the global ones (e.g., NDI). Inferential model comparisons revealed that spline regression models yield a substantial improvement in overall fit for most fiber tracts' FA, MD, RD and NDI (see Table A.3), indicating stronger GA effects in the ePT- and FT-born neonates, when matched for PMA at scan.

3.2. Individual differences in microstructural properties of AVI fiber tracts after preterm birth

To compare the magnitude of individual differences in microstructural properties of AVI fiber tracts between FT and PT infants, we conducted a series of Levene tests for all fiber tracts, DTI and NODDI metrics. After accounting for multiple comparisons, none of the tests remained statistically significant. This indicates that despite several significant associations between microstructural properties in the reconstructed fiber tracts and PT birth (see 3.1.), the extent of individual differences is generally comparable to that of FT neonates. Note that these results correspond to a comparison of the FT neonates with all prematurity groups (PT, vPT and ePT) taken together. Table A.4 in the supplementary material contains the results provided by the Levene tests.

3.3. Preterm birth and the developmental order of AVI fiber tracts

To assess whether PT and FT neonates differ with respect to the developmental order of the reconstructed fiber tracts, we computed between-group ICC coefficients of group-wise averaged DTI and NODDI metrics across fibers. These ICCs indicate the magnitude of between-group agreement in rank order positions of average white matter metrics. The resulting ICC coefficients are displayed in Fig. 3 along with the rank order of each fiber tract in FT and PT neonates. Among all metrics

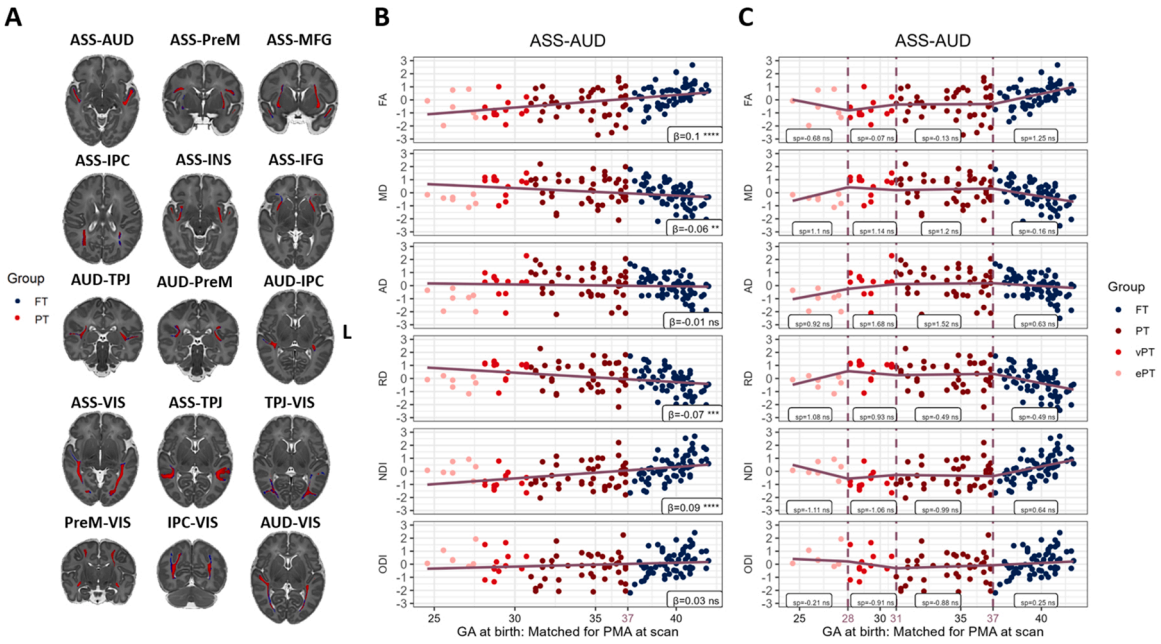

Fig. 2. Statistical models of preterm birth and microstructural properties in neonates matched for PMA at scan. A) FT and PT aggregated tractograms are displayed as overlays on the dHCP 40-week template. One reconstructed fiber tract is chosen to illustrate the relationship between GA at birth and standardized DTI and NODDI metrics in neonates matched for PMA at scan using two models: linear regression (Panel B), and spline regressions (Panel C). Vertical dashed lines represent breaking points dividing the predictor range into ePT, vPT, PT and FT bins. In panels B) and C) *β–weights (regression slopes) and spline coefficients (sp) are displayed on the plots, along with their significance lev*els: ns (non-significant); * ($p < .05$), * * ($p < .01$), * ** ($p < .001$), * ** * ($p < .0001$). VIS – visual areas; AUD – auditory areas; ASS –associative multisensory areas (along the STS); PreM – premotor cortex; MFG – middle frontal gyrus; ACC – anterior cingulate cortex; INS – anterior insula; IPC – inferior parietal cortex; IFG – inferior frontal gyrus; TPJ – temporo-parietal junction.

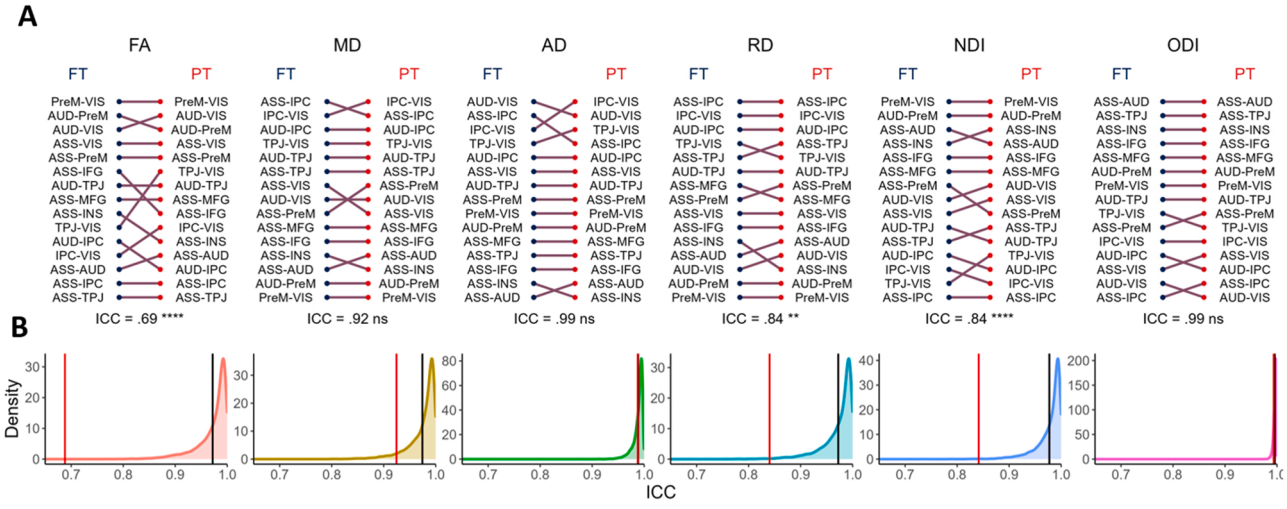

Fig. 3. Between-group correspondence of reconstructed fiber tracts' developmental order. Panel A) For each metric of interest, fiber tracts are arranged in ascending order of group-wise averages. Purple lines indicate between-group differences (non-horizontal lines) or equivalence (horizontal lines) in rank order positions for a given fiber tract. The ICC coefficient as a measure of agreement between FT and PT group-wise averages in fiber metrics is displayed at the bottom, along with their significance levels: ns (non-significant); * ($p < .05$), * * ($p < .01$), * ** ($p < .001$), * ** * ($p < .0001$). Panel B) For each metric of interest, ICC coefficient distributions are simulated via 500 permutations. Statistical significance of the observed ICC coefficient (red vertical line) is given by the proportion of outcomes in the null distribution that is more extreme than the observed ICC coefficient. Black vertical lines represent the mean ICC coefficient across permutations. VIS – visual areas; AUD – auditory areas; ASS –associative multisensory areas (along the STS); PreM – premotor cortex; MFG – middle frontal gyrus; ACC – anterior cingulate cortex; INS – anterior insula; IPC – inferior parietal cortex; IFG – inferior frontal gyrus; TPJ – temporo-parietal junction.

of interest, only FA, RD and NDI showed ICC coefficients substantially smaller than those expected under the null hypothesis. This suggests that at the group level, the developmental order of the reconstructed fiber bundles is considerably different for FA, RD and NDI metrics between PT and FT neonates. AD and ODI exhibit the highest correspondence of the developmental order across groups. This is in line with the results revealed by the regression analysis showing that the association between GA in neonates matched for PMA at scan and AD and ODI was overall not significant. Therefore, only minor differences in developmental order are concluded for these metrics. On the contrary, DTI and NODDI metrics which were associated with prematurity showed lower ICC coefficients. Our findings suggest that at the group level, the rank order of strengths in microstructural properties of the reconstructed fiber tracts is similar across groups for metrics mildly associated with

prematurity and different when this association is strong. In other words, for some microstructural markers, the average developmental order of the reconstructed fiber tracts is associated with prematurity at around term age.

3.4. Preterm birth and fiber tracts' connectivity morphology

To compare tractograms in FT vs. PT groups morphologically, we computed DSCs for each fiber tract across various specificity levels (i.e., within-group spatial agreement, see Section 2.4.3). These are displayed in Fig. 4, Panel A. Average empirical DSCs across specificity levels (red dashed line) reveal a strong spatial similarity between FT and PT infants in all the reconstructed fiber bundles. Specifically, the spatial correspondence exceeded 50% in all cases, 65% in all but one fiber tract (TPJ-VIS) and was highest for the paths linking the associative cortex with the auditory and visual cortices and the TPJ. Considerably lower DSCs were observed for most fiber tracts when no thresholding was performed, likely due to noise induced by within-group inter-individual variability.

Although most DSCs are considerably high, meaningful differences between FT and PT infants are present. To test whether between-group differences were statistically significant, we repeatedly computed DSCs on 500 resampled data sets. Panel B in Fig. 4 depicts the simulated null distribution and the empirical DSCs for three specificity levels in the two fiber tracts with the highest and lowest mean DSCs, respectively. Besides the reconstructed fiber bundles between the associative cortex and the TPJ and the PreM, and between the TPJ and the auditory cortices, all paths were morphologically distinct between PT and FT neonates for at least one level of specificity. These differences are robust for several fiber bundles, such as ASS-AUD and ASS-IFG, indicated by statistical significance irrespective of the extent of the within-group tractograms' spatial overlap. Overall, our findings suggest substantial differences between PT and FT neonates in the morphology of fiber bundles among AVI brain regions.

4. Discussion

Extensive empirical research evinces a variety of sequelae following PT birth even in the absence of apparent brain alterations. These include cognitive and sensory deficits (e.g., Mwaniki et al., 2012; Pascal et al., 2018). Although visual and auditory sequelae have been widely investigated (Arpino et al., 2010; Ream and Lehwald, 2018), there are few studies on AVI. This ability has been related to the development of several cognitive abilities and presumably underlies some of the cognitive and behavioral sequelae associated with prematurity. The present study is a first effort to assess the association between prematurity and fiber tracts linking brain regions documented to be activated in AVI tasks when performed by term born very young infants (e.g., Altvater-Mackensen and Grossmann, 2016; Bristow et al., 2009; Kushnerenko et al., 2008).

4.1. Prematurity and white matter microstructure in AVI fiber tracts

Our findings are mainly in line with the first hypothesis according to which GA at birth and microstructural properties, as assessed by DTI and NODDI metrics, are significantly associated in neonates matched for PMA at scan. Results demonstrated GA at birth to predict higher FA, and NDI and lower MD and RD in AVI fibers when measured at around term age. Higher FA, as well as lower RD (and consequently MD) are regarded as indicators of white matter microstructure development, as they are characteristic during early postnatal development (Akazawa et al., 2016; Feng et al., 2019; Nossin-Manor et al., 2015; Pecheva et al., 2017). Contrarily, the magnitude of prematurity was in general not significantly associated with neurite dispersion (i.e., lower axon coherence), thereby providing a tempting explanation for the non-significant association between GA at birth and AD. ODI positive *β–weights are* likely a consequence of increasing fiber complexity (e.g., crossing, kissing; Batalle et al., 2017). In line with other studies (Chang et al., 2015; Kimpton et al., 2021; Lynch et al., 2020; Mah et al., 2017), our findings indicate that ODI is a less sensitive marker of early white matter microstructure development.

The effect of prematurity on microstructural brain properties can be partly explained by the interruption of the gestational process during fiber connection growth and early premyelination (Back, 2017; Dubois et al., 2014). Additionally, earlier exposure to the extra-uterine environment is likely to affect axonal pruning processes. However, the precise mechanisms underlying observed effects on microstructural model parameters remain debatable (Penn et al., 2016), thus calling for innovative analysis approaches. As a first step toward this aim, in the present study we applied spline regressions to model the association of clinically-defined prematurity groups with metrics of microstructure.

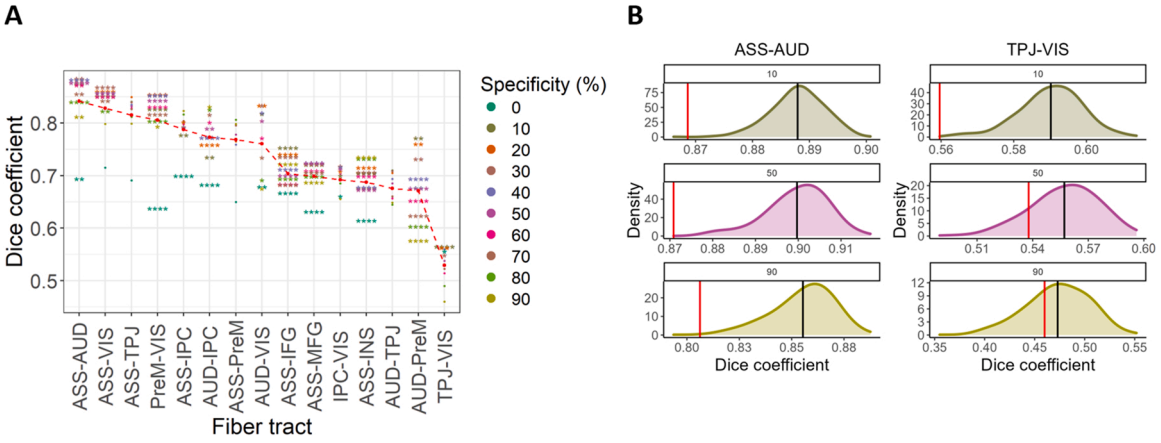

Fig. 4. Between-group spatial correspondence. A) For PT and FT groups independently, individual tractograms were aggregated and thresholded at different levels (i.e., specificity levels). Dice similarity coefficients (DSCs) were computed between groups on the resulting group-wise aggregated masks. The red dashed line represents the mean DSC across specificity levels (empirical DSC means). Dots and asterisks depict statistically non-significant and significant differences across groups, respectively. • (non-significant); * ($p < .05$), * * ($p < .01$), * ** ($p < .001$), * ** * ($p < .0001$). B) The procedure described in A) is repeated on 500 resampled data sets to simulate null distributions. The density function of three specificity levels and two fiber tracts is plotted as example. Statistical significance is given by the proportion of outcomes in the null distribution that is more extreme than the empirical DSC (vertical red line). Black vertical lines represent the mean DSCs in each null distribution. Colored asterisks in A) represent significant DSCs following this principle after adjusting for multiple comparisons. VIS – visual areas; AUD – auditory areas; ASS –associative multisensory areas (along the STS); PreM – premotor cortex; MFG – middle frontal gyrus; ACC – anterior cingulate cortex; INS – anterior insula; IPC – inferior parietal cortex; IFG – inferior frontal gyrus; TPJ – temporo-parietal junction.

Results revealed approximate u-shape-like (for FA and NDI) an inverted u-shape-like relationships (for MD, AD, RD) between DTI and NODDI metrics and GA at birth. These suggest different altered biological processes across the prematurity spectrum. For instance, well-established maturational events show highest susceptibility of oligodendrocytes' precursors to adverse events between 23 and 32 weeks GA (Back, 2017; Volpe, 2009), which renders mid-late PT individuals more resistant.

We reason that at around term age, less developed microstructure comprehended by the in-vivo-reconstructed fiber bundles can be expected in PT individuals. Similar effects on DTI metrics have been observed throughout the brain (Kelly et al., 2016) and particular brain regions, such as the corpus callosum (Dibble et al., 2021; Hasegawa et al., 2011), the optical radiations (Bassi et al., 2008; Weinstein et al., 2016) and the cingulum (Pannek et al., 2020). To our knowledge, no study has directly addressed tract-averaged NODDI metrics in FT and PT neonates at term age. However, cross-sectional studies including neonates born and scanned during the preterm period report an association between prematurity and decreased NDI in major white matter bundles (Kimpton et al., 2021) and throughout the brain (Batalle et al., 2017). Such effect relates primarily to neurite density (e.g., through axonal packing, growth) rather than fiber coherence and highlight the specificity gain encountered in NODDI. Oligodendrocyte and axonal development are two main processes presumably affected in PT individuals. In either case, prematurity effect on microstructure ultimately implies atypical functional communication among brain regions (Penn et al., 2016). This is the first study to provide a microstructural basis for atypical functional architecture among brain areas involved in AVI (Sours et al., 2017) and thus, to provide a likely basic first explanation for PT sequelae observed in several domains, such as language and social cognition.

4.2. Prematurity and individual differences in microstructural properties of AVI fibers

The second hypothesis postulated that prematurity is associated with the magnitude of individual differences in microstructural properties in the reconstructed fiber bundles. Such an effect was expected given the interrupted developmental processes due to PT delivery (Bapat et al., 2014; Blüml et al., 2014), which in addition supposes more variable and prolonged exposure to extrauterine environment by the time of scan. Our results were not in line with this expectation. Same interindividual variance reflects qualitatively similar maturational processes independently on the variable extrauterine environments to which different neonates are exposed. At least this is the case for white matter at the scale captured via microstructural models (e.g., Akazawa et al., 2016; Baldoli et al., 2015), despite absolute differences in DTI and NODDI metrics. However, one methodological challenge potentially limiting the conclusions based on these results is that all PT individuals were grouped together independently of the degree of prematurity. This procedure was needed due to insufficient number of ePT and vPT neonates which would have enabled reliable comparisons among these more differentiated groups. The joint PT group in this study is considered mid-late PT and differs by around three gestation weeks from FT neonates.

4.3. Prematurity and developmental order of AVI fiber tracts

A third aim of the present study was to compare the developmental order of fiber tracts linking brain regions engaged in AVI in FT and PT neonates. We postulated that these groups would show substantial differences. Such direct comparisons lack in the neonatal and prematurity literature in general. In terms of FA, RD, and NDI, the developmental order of the reconstructed fiber tracts at the group level was substantially different between FT and PT neonates. Contrarily, for the remaining metrics studied here, there is not enough evidence to discard a comparable developmental order in FT as compared with PT neonates. We highlight that substantial differences in the developmental order were observed in those microstructural metrics which were associated with the magnitude of prematurity. That is, largest ICC coefficients were found for parameters with less clear associations with GA at birth in linear regression models (AD and ODI). We therefore claim that strong correspondence in developmental order at the group level is partly due to overall little variation observed in our sample at scan time. In other words, stronger differences between FT and PT infants may develop with time, thus being apparent only after more extensive extra-uterine periods.

In the absence of such data however, the similarity of developmental orders based on OD and ODI concurs with studies that report comparable relationships between microstructural properties and PMA shortly after birth in FT and PT infants (Akazawa et al., 2016; Feng et al., 2019; Kersbergen et al., 2014). Arguably, despite disturbances in metabolic and cellular developmental processes induced by earlier exposure to the extrauterine environment (Bapat et al., 2014; Blüml et al., 2014; Chau et al., 2013; Volpe, 2009), larger-scale developmental trajectories are comparable to those observed in FT infants. A few studies employing graph theoretical approaches have found connective properties that are independent of GA at birth (Ball et al., 2014; Batalle et al., 2017), suggesting that some structural connectivity characteristics are indistinguishable between FT and PT neonates. However, these studies did not explicitly focus on the connections of interest for the present study and made use of different connectivity metrics. We interpret our findings as evidence that the average developmental order of the reconstructed fiber bundles is affected by prematurity.

4.4. Spatial similarity in AVI fiber tracts depending on age at birth

Our fourth working hypothesis postulated that reconstructed fiber tracts would exhibit substantial morphological discrepancies between the FT and PT neonates. Our analysis showed that on average across individuals, despite large estimates of spatial overlap (85%), the morphology of the reconstructed fiber tracts is substantially different across groups. Overall, morphological differences were robust even when accounting for interindividual variability, thus supporting our hypothesis.

Recent studies provide a glimpse to innate and early functional connectivity of the brain. There is evidence that by the time of delivery, gross structural architecture is in place, though immature (Smyser et al., 2019). In addition, it has been observed that functional networks comprising primary sensory and motor areas are more mature and exhibit less inter-individual variability as compared with other brain networks. Arguably, analogous structural pathways can be expected to exhibit less inter-individual variability as well. Along with well-established findings on large-scale white matter developmental trajectories (e.g., Gao et al., 2009; Qiu et al., 2015), these previous findings constitute a plausible explanation for the considerable spatial overlap of fiber bundles across groups revealed by the present study. Nevertheless, substantial differences between FT and PT neonates are explicable considering that microstructural properties are reflected on DWI and in turn influence tractography algorithms. Regional and brain volume differences (Keunen et al., 2012), as well as compensatory connectivity mechanisms in PT infants (Ball et al., 2014) are likely to contribute to substantial spatial differences.

Noteworthy, non-significant between-group differences in the path traced between the associative cortex and the TPJ were found. Our previous work revealed a large connective probability between these brain regions in neonates, arguably driven by the importance of multimodal social-related information (Quinones et al., 2022). We speculate that communication between these brain regions is vital from the onset of life and remains unaffected by prematurity in the time around delivery. Our findings indicate that at around term age, spatial attributes of in-vivo reconstructed fiber bundles linking brain regions engaged in AVI are in general substantially different in PT as compared to FT neonates,

with notable exceptions.

4.5. Future directions

The current study suggests that analyzing functional connectivity and behavioral/cognitive measures are crucial future steps to deepen our understanding of AVI and its association with prematurity. Functional connectivity among brain regions engaged in AVI needs to be studied in association with PT birth and microstructural properties. Longitudinal studies involving early life span cohorts are to be planned to include richer developmental and cognitive tests. Importantly, although the present study focused on structural connections among brain regions that have been reported to be active in AVI in very young infants, drawing a direct link between such connections and an AVI ability is only possible on the basis of additional behavioral data. A few exemplary studies have assessed the relationship between brain microstructure and cognitive functions, such as language, memory and a few forms of AVI in adults (Caldinelli et al., 2017; Møller et al., 2021; Mürner-Lavanchy et al., 2018; Zamm et al., 2014). We encourage future research to include behavioral data collected from very young FT and PT infants.

5. Conclusion

A growing body of research demonstrates a widespread of short- and long-lasting cognitive and behavioral sequelae following PT birth. Despite the key role of AVI in early cognitive development, it has received little attention in relation to PT birth, although a handful of behavioral studies have drawn a link between the two. On the basis of previous work on FT neonates, the present study demonstrated that at around term age, prematurity is associated with microstructural properties typically related to less developed white matter in in-vivo reconstructed fiber bundles among brain regions engaged in AVI. Employing DTI and NODDI we concluded that the observed differences relate primarily to neurite density rather than fiber coherence. In general, these fiber bundles were found to differ significantly between FT and PT neonates in terms of spatial attributes. However, inter-individual variability of DTI and NODDI metrics is comparable in the FT and PT groups. Finally, our findings suggest that at the group level, the association between prematurity and atypical developmental order of the analyzed fiber bundles is restricted to a few DTI and NODDI metrics. We conclude that microstructural, morphological and developmental differences in brain connectivity among brain regions engaged in AVI are likely to substantiate deficits in AVI observed later in life.

Funding

The present study was partially funded by the Deutsche Forschungsgemeinschaft (DFG, German Research Foundation; Germany's Excellence Strategy – EXC 2177/1 – Project ID 390895286). Computational resources from the High-Performance Computing Cluster Centre at the Carl von Ossietzky Universität were used to perform neuroimaging analysis. The High-Performance Computing Cluster Centre at the Carl von Ossietzky Universität receives funding from the DFG, Project number 290771637. JFQS was supported through research funds of the School of Medicine and Health Sciences at the Carl von Ossietzky Universität Oldenburg.

Declaration of Competing Interest

The authors declare that they have no known competing financial interests or personal relationships that could have appeared to influence the work reported in this paper.

Data Availability

Preprocessed data analyzed in this study may be obtained via registration to the Developing Human Connectome Project (dHCP); http://www.developingconnectome.org/project/ and provided that access is granted by the project administrators.

Appendix A. Supporting information

Supplementary data associated with this article can be found in the online version at doi:10.1016/j.dcn.2023.101202.

References

Akazawa, K., Chang, L., Yamakawa, R., Hayama, S., Buchthal, S., Alicata, D., Andres, T., Castillo, D., Oishi, K., Skranes, J., Ernst, T., Oishi, K., 2016. Probabilistic maps of the white matter tracts with known associated functions on the neonatal brain atlas: application to evaluate longitudinal developmental trajectories in term-born and preterm-born infants. NeuroImage 128, 167–179. https://doi.org/10.1016/j.neuroimage.2015.12.026.

Altvater-Mackensen, N., Grossmann, T., 2015. Learning to match auditory and visual speech cues: social influences on acquisition of phonological categories. Child Dev. 86 (2), 362–378. https://doi.org/10.1111/cdev.12320.

Altvater-Mackensen, N., Grossmann, T., 2016. The role of left inferior frontal cortex during audiovisual speech perception in infants. NeuroImage 133, 14–20. https://doi.org/10.1016/j.neuroimage.2016.02.061.

Arpino, C., Compagnone, E., Montanaro, M.L., Cacciatore, D., Luca, A., De, Cerulli, A., Girolamo, S., Di, Curatolo, P., 2010. Preterm birth and neurodevelopmental outcome: a review. Child's Nerv. Syst. 26 (9), 1139–1149. https://doi.org/10.1007/s00381-010-1125-y.

Austin, P.C., 2011. An introduction to propensity score methods for reducing the effects of confounding in observational studies. Multivar. Behav. Res. 46 (3), 399–424. https://doi.org/10.1080/00273171.2011.568786.

Back, S.A., 2017. White matter injury in the preterm infant: pathology and mechanisms. Acta Neuropathol. 134 (3), 331–349. https://doi.org/10.1007/s00401-017-1718-6.

Baldoli, C., Scola, E., Della Rosa, P.A., Pontesilli, S., Longaretti, R., Poloniato, A., Scotti, R., Blasi, V., Cirillo, S., Iadanza, A., Rovelli, R., Barera, G., Scifo, P., 2015. Maturation of preterm newborn brains: a fMRI–DTI study of auditory processing of linguistic stimuli and white matter development. Brain Struct. Funct. 220 (6), 3733–3751. https://doi.org/10.1007/s00429-014-0887-5.

Ball, G., Aljabar, P., Zebari, S., Tusor, N., Arichi, T., Merchant, N., Robinson, E.C., Ogundipe, E., Rueckert, D., Edwards, A.D., Counsell, S.J., 2014. Rich-club organization of the newborn human brain. Proc. Natl. Acad. Sci. USA 111 (20), 7456–7461. https://doi.org/10.1073/pnas.1324118111.

Bapat, R., Narayana, P.A., Zhou, Y., Parikh, N.A., 2014. Magnetic resonance spectroscopy at term-equivalent age in extremely preterm infants: Association with cognitive and language development. Pediatr. Neurol. 51 (1), 53–59. https://doi.org/10.1016/j.pediatrneurol.2014.03.011.

Bartha-Doering, L., Alexopoulos, J., Giordano, V., Stelzer, L., Kainz, T., Benavides-Varela, S., Wartenburger, I., Klebermass-Schrehof, K., Olischar, M., Seidl, R., Berger, A., 2019. Absence of neural speech discrimination in preterm infants at term-equivalent age. Dev. Cogn. Neurosci. 39 (April), 100679 https://doi.org/10.1016/j.dcn.2019.100679.

Bassi, L., Ricci, D., Volzone, A., Allsop, J.M., Srinivasan, L., Pai, A., Ribes, C., Ramenghi, L.A., Mercuri, E., Mosca, F., Edwards, A.D., Cowan, F.M., Rutherford, M.A., Counsell, S.J., 2008. Probabilistic diffusion tractography of the optic radiations and visual function in preterm infants at term equivalent age. Brain 131 (2), 573–582. https://doi.org/10.1093/brain/awm327.

Bastiani, M., Andersson, J.L.R., Cordero-Grande, L., Murgasova, M., Hutter, J., Price, A.N., Makropoulos, A., Fitzgibbon, S.P., Hughes, E., Rueckert, D., Victor, S., Rutherford, M., Edwards, A.D., Smith, S.M., Tournier, J.D., Hajnal, J.V., Jbabdi, S., Sotiropoulos, S.N., 2019. Automated processing pipeline for neonatal diffusion MRI in the developing Human Connectome Project. NeuroImage 185, 750–763. https://doi.org/10.1016/j.neuroimage.2018.05.064.

Batalle, D., Hughes, E.J., Zhang, H., Tournier, J.D., Tusor, N., Aljabar, P., Wali, L., Alexander, D.C., Hajnal, J.V., Nosarti, C., Edwards, A.D., Counsell, S.J., 2017. Early development of structural networks and the impact of prematurity on brain connectivity. NeuroImage 149, 379–392. https://doi.org/10.1016/j.neuroimage.2017.01.065.

Behrens, T.E.J., Berg, H.J., Jbabdi, S., Rushworth, M.F.S., Woolrich, M.W., 2007. Probabilistic diffusion tractography with multiple fibre orientations: what can we gain. NeuroImage 34 (1), 144–155. https://doi.org/10.1016/j.neuroimage.2006.09.018.

Berdasco-Muñoz, E., Nazzi, T., Yeung, H.H., 2019. Visual scanning of a talking face in preterm and full-term infants. Dev. Psychol. 55 (7), 1353–1361. https://doi.org/10.1037/dev0000737.

Blüml, S., Wisnowski, J.L., Nelson, M.D., Paquette, L., Panigrahy, A., 2014. Metabolic maturation of white matter is altered in preterm infants. PLoS ONE 9 (1). https://doi.org/10.1371/journal.pone.0085829.

Bristow, D., Dehaene-Lambertz, G., Mattout, J., Soares, C., Gliga, T., Baillet, S., Mangin, J.F., 2009. Hearing faces: how the infant brain matches the face it sees with

the speech it hears. J. Cogn. Neurosci. 21 (5), 905–921. https://doi.org/10.1162/jocn.2009.21076.
Caldinelli, C., Froudist-Walsh, S., Karolis, V., Tseng, C.E., Allin, M.P., Walshe, M., Cuddy, M., Murray, R.M., Nosarti, C., 2017. White matter alterations to cingulum and fornix following very preterm birth and their relationship with cognitive functions. NeuroImage 150 (February), 373–382. https://doi.org/10.1016/j.neuroimage.2017.02.026.
Chang, Y.S., Owen, J.P., Pojman, N.J., Thieu, T., Bukshpun, P., Wakahiro, M.L.J., Berman, J.I., Roberts, T.P.L., Nagarajan, S.S., Sherr, E.H., Mukherjee, P., 2015. White matter changes of neurite density and fiber orientation dispersion during human brain maturation. PLoS ONE 10 (6). https://doi.org/10.1371/journal.pone.0123656.
Chau, V., Synnes, A., Grunau, R.E., Poskitt, K.J., Brant, R., Miller, S.P., 2013. Abnormal brain maturation in preterm neonates associated with adverse developmental outcomes. Neurology 81 (24), 2082–2089. https://doi.org/10.1212/01.wnl.0000437298.43688.b9.
Coker-Bolt, P., Barbour, A., Moss, H., Tillman, J., Humphries, E., Ward, E., Brown, T., Jenkins, D., 2016. Correlating early motor skills to white matter abnormalities in preterm infants using diffusion tensor imaging. J. Pediatr. Rehabil. Med. 9 (3), 185–193. https://doi.org/10.3233/PRM-160380.
Curtindale, L.M., Bahrick, L.E., Lickliter, R., Colombo, J., 2019. Effects of multimodal synchrony on infant attention and heart rate during events with social and nonsocial stimuli. J. Exp. Child Psychol. 178, 283–294. https://doi.org/10.1016/j.jecp.2018.10.006.
Dibble, M., Ang, J.Z., Mariga, L., Molloy, E.J., Bokde, A.L.W., 2021. Diffusion tensor imaging in very preterm, moderate-late preterm and term-born neonates: a systematic review. J. Pediatr. 232 (48–58), e3 https://doi.org/10.1016/j.jpeds.2021.01.008.
Dubois, J., Dehaene-Lambertz, G., Kulikova, S., Poupon, C., Hüppi, P.S., Hertz-Pannier, L., 2014. The early development of brain white matter: a review of imaging studies in fetuses, newborns and infants. Neuroscience 276, 48–71. https://doi.org/10.1016/j.neuroscience.2013.12.044.
Elburg, R.M. Van, Oosterlaan, J., 2019. Social adjustment in adolescents born very preterm: evidence for a cognitive basis of social problems. J. Pediatr. 213 (66–73), e1 https://doi.org/10.1016/j.jpeds.2019.06.045.
Faria, A.V., Zhang, J., Oishi, K., Li, X., Jiang, H., Akhter, K., Hermoye, L., Lee, S.K., Hoon, A., Stashinko, E., Miller, M.I., van Zijl, P.C.M., Mori, S., 2010. Atlas-based analysis of neurodevelopment from infancy to adulthood using diffusion tensor imaging and applications for automated abnormality detection. NeuroImage 52 (2), 415–428. https://doi.org/10.1016/j.neuroimage.2010.04.238.
Fellman, V., Kushnerenko, E., Mikkola, K., Ceponiene, R., Leipälä, J., Näätänen, R., 2004. Atypical auditory event-related potentials in preterm infants during the first year of life: A possible sign of cognitive dysfunction. Pediatr. Res. 56 (2), 291–297. https://doi.org/10.1203/01.PDR.0000132750.97066.B9.
Feng, L., Li, H., Oishi, K., Mishra, V., Song, L., Peng, Q., Ouyang, M., Wang, J., Slinger, M., Jeon, T., Lee, L., Heyne, R., Chalak, L., Peng, Y., Liu, S., Huang, H., 2019. Age-specific gray and white matter DTI atlas for human brain at 33, 36 and 39 postmenstrual weeks. NeuroImage 185, 685–698. https://doi.org/10.1016/j.neuroimage.2018.06.069.
Fenoglio, A., Georgieff, M.K., Elison, J.T., 2017. Social brain circuitry and social cognition in infants born preterm. J. Neurodev. Disord. 9 (1), 1–16. https://doi.org/10.1186/s11689-017-9206-9.
Fick, R.H.J., Wassermann, D., Deriche, R., 2019. The dmipy toolbox: diffusion MRI multi-compartment modeling and microstructure recovery made easy. Front. Neuroinformatics 13, 1–26. https://doi.org/10.3389/fninf.2019.00064.
Flom, R., Bahrick, L.E., 2012. The development of infant discrimination of affect in multimodal and unimodal stimulation: the role of intersensory redundancy. Bone 23 (1), 1–7. https://doi.org/10.1038/jid.2014.371.
Fukutomi, H., Glasser, M.F., Murata, K., Akasaka, T., Fujimoto, K., Yamamoto, T., Autio, J.A., Okada, T., Togashi, K., Zhang, H., Essen, D.C., Van, Hayashi, T., 2019. Diffusion tensor model links to neurite orientation dispersion and density imaging at high b-value in cerebral cortical gray matter. Sci. Rep. 6–7. https://doi.org/10.1038/s41598-019-48671-7.
Gao, W., Lin, W., Chen, Y., Gerig, G., Smith, J.K., Jewells, V., Gilmore, J.H., 2009. Temporal and spatial development of axonal maturation and myelination of white matter in the developing brain. Am. J. Neuroradiol. 30 (2), 290–296. https://doi.org/10.3174/ajnr.A1363.
Geng, X., Gouttard, S., Sharma, A., Gu, H., Styner, M., Lin, W., Gerig, G., Gilmore, J.H., 2012. Quantitative tract-based white matter development from birth to age 2years. NeuroImage 61 (3), 542–557. https://doi.org/10.1016/j.neuroimage.2012.03.057.
Glasser, M.F., Coalson, T.S., Robinson, E.C., Hacker, C.D., Harwell, J., Yacoub, E., Ugurbil, K., Andersson, J., Beckmann, C.F., Jenkinson, M., Smith, S.M., Van Essen, D. C., 2016. A multi-modal parcellation of human cerebral cortex. Nature 536 (7615), 171–178. https://doi.org/10.1038/nature18933.
Grossmann, T., 2015. The development of social brain functions in infancy. Psychol. Bull. 141 (6), 1266–1287. https://doi.org/10.1037/bul0000002.
Hasegawa, T., Yamada, K., Morimoto, M., Morioka, S., Tozawa, T., Isoda, K., Murakami, A., Chiyonobu, T., Tokuda, S., Nishimura, A., Nishimura, T., Hosoi, H., 2011. Development of corpus callosum in preterm infants is affected by the prematurity: In vivo assessment of diffusion tensor imaging at term-equivalent age. Pediatr. Res. 69 (3), 249–254. https://doi.org/10.1203/PDR.0b013e3182084e54.
Healy, E., Reichenberg, A., Nam, K.W., Allin, M.P.G., Walshe, M., Rifkin, L., Murray, S.R. M., Nosarti, C., 2013. Preterm birth and adolescent social functioning-alterations in emotion-processing brain areas. J. Pediatr. 163 (6), 1596–1604. https://doi.org/10.1016/j.jpeds.2013.08.011.
Hickok, G., Rogalsky, C., Matchin, W., Basilakos, A., Cai, J., Pillay, S., Ferrill, M., Mickelsen, S., Anderson, S.W., Love, T., Binder, J., Fridriksson, J., 2018. Neural networks supporting audiovisual integration for speech: a large-scale lesion study. Cortex 103, 360–371. https://doi.org/10.1016/j.cortex.2018.03.030.
Imafuku, M., Kawai, M., Niwa, F., Shinya, Y., Myowa, M., 2019. Audiovisual speech perception and language acquisition in preterm infants: a longitudinal study. Early Hum. Dev. 128 (February 2018), 93–100. https://doi.org/10.1016/j.earlhumdev.2018.11.001.
Jansson-Verkasalo, E., Ruusuvirta, T., Huotilainen, M., Alku, P., Kushnerenko, E., Suominen, K., Rytky, S., Luotonen, M., Kaukola, T., Tolonen, U., Hallman, M., 2010. Atypical perceptual narrowing in prematurely born infants is associated with compromised language acquisition at 2 years of age. BMC Neurosci. *11*. https://doi.org/10.1186/1471-2202-11-88.
Jo, H.M., Cho, H.K., Jang, S.H., Yeo, S.S., Lee, E., Kim, H.S., Son, S.M., 2012. A comparison of microstructural maturational changes of the corpus callosum in preterm and full-term children: a diffusion tensor imaging study. Neuroradiology 54 (9), 997–1005. https://doi.org/10.1007/s00234-012-1042-8.
Jones, K.M., Champion, P.R., Woodward, L.J., 2013. Social competence of preschool children born very preterm. Early Hum. Dev. 89 (10), 795–802. https://doi.org/10.1016/j.earlhumdev.2013.06.008.
Kamiya, K., Hori, M., Aoki, S., 2020. NODDI in clinical research. J. Neurosci. Methods 346, 108908. https://doi.org/10.1016/j.jneumeth.2020.108908.
Kelly, C.E., Cheong, J.L.Y., Gabra Fam, L., Leemans, A., Seal, M.L., Doyle, L.W., Anderson, P.J., Spittle, A.J., Thompson, D.K., 2016. Moderate and late preterm infants exhibit widespread brain white matter microstructure alterations at term-equivalent age relative to term-born controls. Brain Imaging Behav. 10 (1), 41–49. https://doi.org/10.1007/s11682-015-9361-0.
Kerr-Wilson, C.O., MacKay, D.F., Smith, G.C.S., Pell, J.P., 2012. Meta-analysis of the association between preterm delivery and intelligence. J. Public Health 34 (2), 209–216. https://doi.org/10.1093/pubmed/fdr024.
Kersbergen, K.J., Leemans, A., Groenendaal, F., van der Aa, N.E., Viergever, M.A., de Vries, L.S., Benders, M.J.N.L., 2014. Microstructural brain development between 30 and 40 weeks corrected age in a longitudinal cohort of extremely preterm infants. NeuroImage 103, 214–224. https://doi.org/10.1016/j.neuroimage.2014.09.039.
Keunen, K., Kersbergen, K.J., Groenendaal, F., Isgum, I., Vries, L.S., De, Benders, M.J.N. L., 2012. Brain tissue volumes in preterm infants: prematurity, perinatal risk factors and neurodevelopmental outcome: A systematic review. J. Matern. Fetal. Neonatal. Med. 25 (1), 89–100. https://doi.org/10.3109/14767058.2012.664343.
Kidowaki, S., Morimoto, M., Yamada, K., Sakai, K., Zuiki, M., Maeda, H., Yamashita, S., Morita, T., Hasegawa, T., Chiyonobu, T., Tokuda, S., Hosoi, H., 2017. Longitudinal change in white matter in preterm infants without magnetic resonance imaging abnormalities: Assessment of serial diffusion tensor imaging and their relationship to neurodevelopmental outcomes. Brain Dev. 39 (1), 40–47. https://doi.org/10.1016/j.braindev.2016.07.007.
Kimpton, J.A., Batalle, D., Barnett, M.L., Hughes, E.J., Chew, A.T.M., Falconer, S., Tournier, J.D., Alexander, D., Zhang, H., Edwards, A.D., Counsell, S.J., 2021. Diffusion magnetic resonance imaging assessment of regional white matter maturation in preterm neonates. Neuroradiology 63 (4), 573–583. https://doi.org/10.1007/s00234-020-02584-9.
Kushnerenko, E., Teinonen, T., Volein, A., Csibra, G., 2008. Electrophysiological evidence of illusory audiovisual speech percept in human infants. Proc. Natl. Acad. Sci. 105 (32), 11442–11445. https://doi.org/10.1073/pnas.0804275105.
Loe, I.M., Adams, J.N., Feldman, H.M., 2019. Executive function in relation to white matter in preterm and full term children. Front. Pediatr. 6 (JAN), 1–7. https://doi.org/10.3389/fped.2018.00418.
Lynch, K.M., Cabeen, R.P., Toga, A.W., Clark, K.A., 2020. Magnitude and timing of major white matter tract maturation from infancy through adolescence with NODDI. NeuroImage 212 (January), 116672. https://doi.org/10.1016/j.neuroimage.2020.116672.
Mah, A., Geeraert, B., Lebel, C., 2017. Detailing neuroanatomical development in late childhood and early adolescence using NODDI. PLOS ONE 12 (8), e0182340. https://doi.org/10.1371/journal.pone.0182340.
Makropoulos, A., Robinson, E.C., Schuh, A., Wright, R., Fitzgibbon, S., Bozek, J., Counsell, S.J., Steinweg, J., Vecchiato, K., Passerat-Palmbach, J., Lenz, G., Mortari, F., Tenev, T., Duff, E.P., Bastiani, M., Cordero-Grande, L., Hughes, E., Tusor, N., Tournier, J.D., Rueckert, D., 2018. The developing human connectome project: a minimal processing pipeline for neonatal cortical surface reconstruction. NeuroImage 173, 88–112. https://doi.org/10.1016/j.neuroimage.2018.01.054.
Marcus, D.S., Harwell, J., Olsen, T., Hodge, M., Glasser, M.F., Prior, F., Jenkinson, M., Laumann, T., Curtiss, S.W., Van Essen, D.C., 2011. Informatics and data mining tools and strategies for the human connectome project. Front. Neuroinformatics 5, 1–12. https://doi.org/10.3389/fninf.2011.00004.
Mccunn, P., Gilbert, K.M., Zeman, P., Li, A.X., Strong, M.J., Khan, R., Bartha, R., 2019. Reproducibility of neurite orientation dispersion and density imaging (NODDI) in rats at 9. 4 Tesla. PLoS ONE 14 (4), 1–14. https://doi.org/10.1371/journal pone.0215974.
Mileva, M., Tompkinson, J., Watt, D., Burton, A.M., 2018. Audio-visual integration in social evaluation. J. Exp. Psychol. Hum. Percept. Perform. 44 (1), 128–138.
Miller, S.P., Ferriero, D.M., 2009. From selective vulnerability to vonnectivity: insights from newborn brain imaging. Trends Neurosci. 32 (9), 496–505. https://doi.org/10.1016/j.tins.2009.05.010.
Miller, S.P., Vigneron, D.B., Henry, R.G., Bohland, M.A., Ceppi-Cozzio, C., Hoffman, C., Newton, N., Partridge, J.C., Ferriero, D.M., Barkovich, A.J., 2002. Serial quantitative diffusion tensor MRI of the premature brain: development in newborns with and without injury. J. Magn. Reson. Imaging 16 (6), 621–632. https://doi.org/10.1002/jmri.10205.

Møller, C., Villarreal, E.A.G., Hansen, N.C., 2021. Audiovisual structural connectivity in musicians and non - musicians: a cortical thickness and diffusion tensor imaging study. Sci. Rep. 11 (1), 1–14. https://doi.org/10.1038/s41598-021-83135-x.

Monson, B.B., Eaton-Rosen, Z., Kapur, K., Liebenthal, E., Brownell, A., Smyser, C.D., Rogers, C.E., Inder, T.E., Warfield, S.K., Neil, J.J., 2018. Differential rates of perinatal maturation of human primary and nonprimary auditory cortex. ENeuro 5 (1), 1–12. https://doi.org/10.1523/ENEURO.0380-17.2017.

Mürner-Lavanchy, I.M., Kelly, C.E., Reidy, N., Doyle, L.W., Lee, K.J., Inder, T., Thompson, D.K., Morgan, A.T., Anderson, P.J., 2018. White matter microstructure is associated with language in children born very preterm. NeuroImage Clin. 20, 808–822. https://doi.org/10.1016/j.nicl.2018.09.020.

Mwaniki, M.K., Atieno, M., Lawn, J.E., Newton, C.R.J.C., 2012. Long-term neurodevelopmental outcomes after intrauterine and neonatal insults: a systematic review. Lancet 379 (9814), 445–452. https://doi.org/10.1016/S0140-6736(11)61577-8.

Navarra, R., Sestieri, C., Conte, E., Salomone, R., Mattei, P.A., Romani, G.L., Domizio, S., Caulo, M., 2016. Perinatal MRI diffusivity is related to early assessment of motor performance in preterm neonates. Neuroradiol. J. 29 (2), 137–145. https://doi.org/10.1177/1971400915628019.

Nossin-Manor, R., Card, D., Raybaud, C., Taylor, M.J., Sled, J.G., 2015. Cerebral maturation in the early preterm period-A magnetization transfer and diffusion tensor imaging study using voxel-based analysis. NeuroImage 112, 30–42. https://doi.org/10.1016/j.neuroimage.2015.02.051.

O'Donnell, L.J., Westin, C.-F., 2011. An introduction to diffusion tensor image analysis. Neurosurg. Clin. North Am. 22 (2), 185–196. https://doi.org/10.1016/j.nec.2010.12.004.

Pannek, K., George, J.M., Boyd, R.N., Colditz, P.B., Rose, S.E., Fripp, J., 2020. Brain microstructure and morphology of very preterm-born infants at term equivalent age: associations with motor and cognitive outcomes at 1 and 2 years. NeuroImage 221, 117163. https://doi.org/10.1016/j.neuroimage.2020.117163.

Pascal, A., Govaert, P., Oostra, A., Naulaers, G., Ortibus, E., Van den Broeck, C., 2018. Neurodevelopmental outcome in very preterm and very-low-birthweight infants born over the past decade: a meta-analytic review. Dev. Med. Child Neurol. 60 (4), 342–355. https://doi.org/10.1111/dmcn.13675.

Pavaine, J., Young, J.M., Morgan, B.R., Shroff, M., Raybaud, C., Taylor, M.J., 2016. Diffusion tensor imaging-based assessment of white matter tracts and visual-motor outcomes in very preterm neonates. Neuroradiology 58 (3), 301–310. https://doi.org/10.1007/s00234-015-1625-2.

Pecheva, D., Yushkevich, P., Batalle, D., Hughes, E., Aljabar, P., Wurie, J., Hajnal, J.V., Edwards, A.D., Alexander, D.C., Counsell, S.J., Zhang, H., 2017. A tract-specific approach to assessing white matter in preterm infants. NeuroImage 157 (March), 675–694. https://doi.org/10.1016/j.neuroimage.2017.04.057.

Penn, A.A., Gressens, P., Fleiss, B., Back, S.A., Gallo, V., 2016. Controversies in preterm brain injury. Neurobiol. Dis. 92 (Part A), 90–101. https://doi.org/10.1016/j.nbd.2015.10.012.

Pickens, J., Field, T., Nawrocki, T., Martinez, A., Soutullo, D., Gonzalez, J., 1994. Full-term and preterm infants' perception of face-voice synchrony. Infant Behav. Dev. 17 (4), 447–455. https://doi.org/10.1016/0163-6383(94)90036-1.

Qiu, A., Mori, S., Miller, M.I., 2015. Diffusion tensor imaging for understanding brain development in early life. Annu. Rev. Psychol. 66 (1), 853–876. https://doi.org/10.1146/annurev-psych-010814-015340.

Quinones, J.F., Pavan, T., Liu, X., Thiel, C.M., Heep, A., Hildebrandt, A., 2022. Fiber tracing and microstructural characterization among audiovisual integration brain regions in neonates compared with young adults. NeuroImage 254, 119141. https://doi.org/10.1016/j.neuroimage.2022.119141.

R Core Team (2022). R: A language and environment for statistical computing. R Foundation for Statistical Computing, Vienna, Austria. URL https://www.R-project.org/.

Ream, M.A., Lehwald, L., 2018. Neurologic consequences of preterm birth. Curr. Neurol. Neurosci. Rep. 18 (8), 48. https://doi.org/10.1007/s11910-018-0862-2.

Robinson, E.C., Jbabdi, S., Glasser, M.F., Andersson, J., Burgess, G.C., Harms, M.P., Smith, S.M., Van Essen, D.C., Jenkinson, M., 2014. MSM: a new flexible framework for multimodal surface matching. NeuroImage 100, 414–426. https://doi.org/10.1016/j.neuroimage.2014.05.069.

Robinson, E.C., Garcia, K., Glasser, M.F., Chen, Z., Coalson, T.S., Makropoulos, A., Bozek, J., Wright, R., Schuh, A., Webster, M., Hutter, J., Price, A., Cordero Grande, L., Hughes, E., Tusor, N., Bayly, P.V., Van Essen, D.C., Smith, S.M., Edwards, A.D., Rueckert, D., 2018. Multimodal surface matching with higher-order smoothness constraints. NeuroImage 167, 453–465. https://doi.org/10.1016/j.neuroimage.2017.10.037.

Rose, S.E., Hatzigeorgiou, X., Strudwick, M.W., Durbridge, G., Davies, P.S.W., Colditz, P.B., 2008. Altered white matter diffusion anisotropy in normal and preterm infants at term-equivalent age. Magn. Reson. Med. 767, 761–767. https://doi.org/10.1002/mrm.21689.

Smyser, C.D., Wheelock, M.D., Limbrick, D.D., Neil, J.J., 2019. Neonatal brain injury and aberrant connectivity. NeuroImage 185 (June 2018), 609–623. https://doi.org/10.1016/j.neuroimage.2018.07.057.

Sours, C., Raghavan, P., Foxworthy, W.A., Meredith, M.A., El Metwally, D., Zhuo, J., Gilmore, J.H., Medina, A.E., Gullapalli, R.P., 2017. Cortical multisensory connectivity is present near birth in humans. Brain Imaging Behav. 11 (4), 1207–1213. https://doi.org/10.1007/s11682-016-9586-6.

Stipdonk, L.W., Franken, M.C.J.P., Dudink, J., 2018. Language outcome related to brain structures in school-aged preterm children: a systematic review. PLoS One 13 (6), 1–16. https://doi.org/10.1371/journal.pone.0196607.

Tariq, M., Schneider, T., Alexander, D.C., Gandini Wheeler-Kingshott, C.A., Zhang, H., 2016. Bingham-NODDI: mapping anisotropic orientation dispersion of neurites using diffusion MRI. NeuroImage 133, 207–223. https://doi.org/10.1016/j.neuroimage.2016.01.046.

Teinonen, T., Aslin, R.N., Alku, P., Csibra, G., 2008. Visual speech contributes to phonetic learning in 6-month-old infants. Cognition 108 (3), 850–855. https://doi.org/10.1016/j.cognition.2008.05.009.

Thorgeirsson, S.S., Atlas, S.A., Boobis, A.R., Felton, J.S., 1979. Recommended definitions, terminology and format for statistical tables related to the perinatal perios and use of a new certificate for cause of perinatal deaths. In: Biochemical Pharmacology, 28. WHO, pp. 217–226. https://doi.org/10.1016/0006-2952(79)90507-0.

Volpe, J.J., 2009. Brain injury in premature infants: a complex amalgam of destructive and developmental disturbances. Lancet Neurol. 8 (1), 110–124. https://doi.org/10.1016/S1474-4422(08)70294-1.

Weinstein, M., Ben-Sira, L., Moran, A., Berger, I., Marom, R., Geva, R., Gross-Tsur, V., Leitner, Y., Ben Bashat, D., 2016. The motor and visual networks in preterm infants: An fMRI and DTI study. Brain Res. 1642, 603–611. https://doi.org/10.1016/j.brainres.2016.04.052.

Yang, Y., Hui, Y., Li, J., Xu, M., Bi, H., 2020. An audiovisual integration deficit underlies reading failure in nontransparent writing systems: an fMRI study of Chinese children with dyslexia. J. Neurolinguist. 54, 100884 https://doi.org/10.1016/j.jneuroling.2019.100884.

Yao, A., Cheng, D., Pan, I., Kitamura, F., 2020. Deep learning in neuroradiology: a systematic review of current algorithms and approaches for the new wave of imaging technology. Radiol.: Artif. Intell. 2 (2), e190026 https://doi.org/10.1148/ryai.2020190026.

Zamm, A., Schlaug, G., Eagleman, D.M., Loui, P., 2014. Pathways to seeing music: enhanced structural connectivity in colored-music synesthesia. NeuroImage 74 (617), 359–366. https://doi.org/10.1016/j.neuroimage.2013.02.024.

Zhang, H., Schneider, T., Wheeler-Kingshott, C.A., Alexander, D.C., 2012. NODDI: practical in vivo neurite orientation dispersion and density imaging of the human brain. NeuroImage 61 (4), 1000–1016. https://doi.org/10.1016/j.neuroimage.2012.03.072.

Zhou, H., Cheung, E.F.C., Chan, R.C.K., 2020. Audiovisual temporal integration: cognitive processing, neural mechanisms, developmental trajectory and potential interventions. Neuropsychologia 140, 107396. https://doi.org/10.1016/j.neuropsychologia.2020.107396.